

Critical Adsorption on Defects in Ising Magnets and Binary Alloys

Andreas Hanke*

Fachbereich Physik, Bergische Universität Wuppertal, D-42097 Wuppertal, Germany

(Received 26 July 1999)

Long-range correlations in a magnet close to its critical point or in a binary alloy close to a continuous order-disorder transition can substantially enhance the effect of local perturbations. It is demonstrated using a position-space renormalization procedure that quasi-one-dimensional defects which break the symmetry of the order parameter have pronounced effects: They cause long-range critical adsorption profiles and give rise to new universal critical exponents, which are identified and calculated using field-theoretical methods.

PACS numbers: 64.60.Fr, 05.50.+q, 61.72.Lk, 68.35.Rh

Near a second order phase transition, fluctuations and correlations of the order parameter over large length scales dominate the behavior of the system. The modern theory of critical phenomena is able to identify and to explain the ensuing universal properties by means of the renormalization group [1]. The *bulk* universality class of a particular system is determined by a few gross features only, such as the space dimension and the symmetries of the order parameter, and shows up by a set of universal critical exponents [1].

As a starting point for a theoretical description, one commonly deals with translationally invariant systems of an infinite extent. However, experimental systems such as magnets or binary alloys deviate from this idealized picture in important aspects. On the one hand, they are confined by *surfaces*. The corresponding surface critical behavior has been investigated with remarkable success [2–4]. This theoretical advance is complemented by the increasing quality of the available x-ray probes, which allow quantitative experimental tests of the predictions for the local critical properties [5].

On the other hand, real crystals exhibit a wealth of different types of internal *defects* [6,7]. The emphasis in this Letter is on defects which locally break the symmetry of the order parameter. It is demonstrated that near the bulk critical temperature T_c , a quasi-one-dimensional defect (line defect) gives rise to *critical adsorption*, i.e., long-range adsorption profiles of the preferred phase. This phenomenon may be part of the explanation for, e.g., the anomalous scattering of light observed near line dislocations in NH_4Br crystals [8]. While for a symmetry breaking defect plane the analogous phenomenon is equivalently described by critical adsorption on a confining wall [2,3] on each side of the plane, it turns out that a point defect corresponds to an irrelevant perturbation in a renormalization group sense. Critical adsorption on a line defect represents a new universality class. The main results derived here are the predictions for the corresponding critical exponents shown in Table I. They are argued to be universal and thus allow unambiguous tests.

A simple lattice model which describes a defect in a magnet or in a binary alloy is given by an Ising-type

model (compare Ref. [4]) with statistical Boltzmann weight $\exp(-\mathcal{H}\{s\})$, where

$$\begin{aligned} \mathcal{H}\{s\} = & -K \sum_{\langle ij \rangle} s_i s_j - K_{\perp} \sum_{\langle i\alpha \rangle} s_i s_{\alpha} - K_s \sum_{\langle \alpha\beta \rangle} s_{\alpha} s_{\beta} \\ & - H \sum_i s_i - H_s \sum_{\alpha} s_{\alpha}. \end{aligned} \quad (1)$$

$s_i = \pm 1$ are spin variables on the sites i of a Bravais lattice. In the case of a binary alloy, the numbers $s_i = \pm 1$ specify whether the site i is occupied by species A or species B. The defect consists of a single lattice site (point defect), a row of sites (line defect), or a plane of sites (defect plane). Spins with indices i and j are located off the defect and spins with indices α and β are located on the defect. The brackets $\langle \rangle$ denote nearest neighbor pairs of spins. The fields H and H_s act on spins off and on the defect, respectively. In the case of a ferromagnet, for which the couplings K , K_{\perp} , and K_s are positive, the field H_s represents the local symmetry breaking perturbation. Within the present theoretical approach this situation is also generic for an antiferromagnet or a binary alloy, for which K , K_{\perp} , and K_s are negative [4] and H and H_s represent nonordering fields. In order to illustrate this point, consider an antiferromagnet with bcc lattice and a local field acting on the spins in a row along one of the primitive vectors of one of its *sublattices*; by tracing over the spins of the other sublattice, one ends up at a ferromagnet with effective couplings on a simple cubic lattice, and a line defect along one of its primitive vectors.

TABLE I. Numerical values of universal critical exponents associated with critical adsorption on a line defect [see Eqs. (4) and (5)]. D is the space dimension; $D = 4$ corresponds to the mean-field approximation. The values for critical adsorption on a planar wall are shown for comparison.

	Line defect, $D = 4$	$D = 3$	Planar wall, $D = 3$
η_{\parallel}	$2\sqrt{3}$	1.77 ± 0.05	5
η_{\perp}	$\sqrt{3}$	0.91 ± 0.03	2.518
β_1	$\frac{1}{2}(1 + \sqrt{3})$	0.84 ± 0.05	1.887
γ_1	$1 - \frac{1}{2}\sqrt{3}$	0.72 ± 0.05	-0.326
δ_1	$3/(1 + \sqrt{3})$	1.86 ± 0.10	0.827

The global phase diagram corresponding to the lattice model in Eq. (1) is most directly revealed by a position-space renormalization procedure. In the case of an Ising model with a free surface the so-called Migdal-Kadanoff scheme [9] has proved to exhibit some advantageous features [10]. In particular, the Migdal-Kadanoff scheme reproduces the phase diagram of an Ising model with a free surface for different and even noninteger values of the space dimension D [10]. For the present case, it turns out to be very helpful and instructive to study the lattice model in Eq. (1) not only for different space dimensions D , but also for different internal dimensions of the defect. This can be accomplished by considering the dimension

d of the subspace perpendicular to the defect as a second control parameter. The internal dimension of the defect thus equals $D - d$. (The freedom to vary both D and d becomes essential for calculating the critical exponents shown in Table I; see below.) In space dimension $D = 3$ exists a *critical adsorption fixed point* [2,3] in the case of a line defect, i.e., $(D, d) = (3, 2)$, while such a fixed point is absent in the case of a point defect, i.e., $(D, d) = (3, 3)$. In order to see this it is sufficient to consider a ferromagnet with simple cubic lattice and a defect oriented along (one of) its primitive vectors, and to set $K_{\perp} = K$ and $H = 0$ in Eq. (1). Generalizing the method described in Ref. [10], this yields the flow equations for the renormalized parameters $K(l)$, $K_s(l)$, and $H_s(l)$:

$$\begin{aligned} \frac{dK}{dl} &= (D - 1)K + \frac{1}{2} \sinh(2K) \ln[\tanh(K)], \\ \frac{dK_s}{dl} &= (D - 1)K_s + d(K - K_s) + \frac{1}{2} \sinh(2K_s) \ln[\tanh(K_s)] \\ &\quad - \frac{H_s^2}{4(D - d)^2} [\exp(4K_s) - 1] \{1 + \sinh(2K_s) \ln[\tanh(K_s)]\} + \mathcal{O}(H_s^4), \quad d < D, \\ \frac{dH_s}{dl} &= H_s \{D - d - 1 - \sinh(2K_s) \ln[\tanh(K_s)]\} + \mathcal{O}(H_s^2). \end{aligned} \quad (2)$$

Integrating these flow equations to $l = \infty$ drives the system towards various fixed points which reflect the behavior on large length scales. The first Eq. (2) is the flow equation for the coupling K of the isotropic Ising model, where the condition $dK/dl = 0$ yields the value K^C corresponding to the bulk critical fixed point, as a function of D [10]. Figure 1 shows the behavior of $H_s(l)$ and $K_s(l)$ for $K = K^C$ for a line defect and for a point defect. Evidently, a line defect with nonzero H_s drives the system towards the critical adsorption fixed point $K_s = 0$, $H_s = \infty$ on large length scales.

The flow equations in Eq. (2) can be expected to be only qualitatively correct. However, they yield the behavior of $K(l)$, $K_s(l)$, and $H_s(l)$ for *arbitrary* values of both D and d . This is illustrated in Fig. 2, which on the (D, d) plane shows the location of defect planes, line defects, and point defects. Within the region below the line $d = D - 1 - \sinh(2K_s^C) \ln[\tanh(K_s^C)]$ (dotted line in Fig. 2), with $K_s^C = K^C$ depending on D , $H_s(l)$ is *relevant*, i.e., grows for $l \rightarrow \infty$ (compare Fig. 1). The shape of the dotted line in Fig. 2 is confirmed quite well by the line $d = D - \beta/\nu$ (dashed line in Fig. 2), where $\beta(D)$ and $\nu(D)$ are standard bulk critical exponents [11], below which the defects are relevant perturbations according to arguments based on a special type of operator product expansion [12]. Above the dashed line the defects are irrelevant perturbations, i.e., the system behaves bulklike.

The emphasis of the remaining part of this work is on a line defect in order to calculate the critical exponents shown in Table I. Having established by means of the lattice model in Eq. (1) that the line field H_s is indeed relevant on large length scales, it is convenient to consider

the corresponding continuum description at the critical adsorption fixed point. Here it is important to note that, even if absent *a priori*, such a line field can be induced *effectively* by the coarse graining procedure starting, e.g., from an Ising antiferromagnet with a suitably oriented line dislocation, or topological defect, in the presence of a

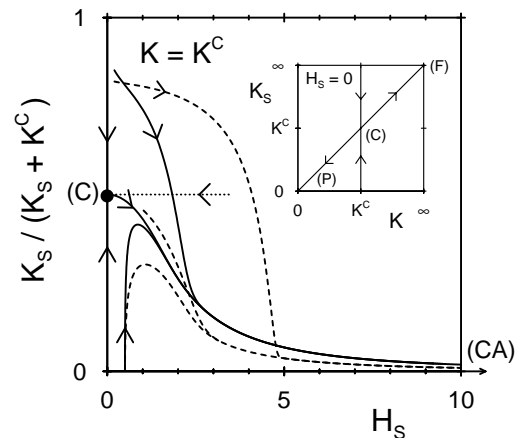


FIG. 1. Flow trajectories $[H_s(l), K_s(l)]$ for critical bulk coupling $K = K^C$ and $H = 0$ for a line defect in the space ($D = 3$ and $d = 2$, solid lines), a line defect in a plane ($D = 2$ and $d = 1$, dashed lines), and a point defect (any D with $d = D$ and K_s set to K^C , dotted line) [see Eqs. (1) and (2)]. For a line defect with $H_s > 0$ the trajectories tend to the critical adsorption fixed point (CA), whereas for a point defect with $H_s > 0$ they tend to the bulk critical point (C). Inset: $[K(l), K_s(l)]$ for a line defect with $H_s = 0$ the deviation $K_s - K$ is irrelevant and the fixed points are bulklike: bulk critical (C), ferromagnetic (F), and paramagnetic (P).

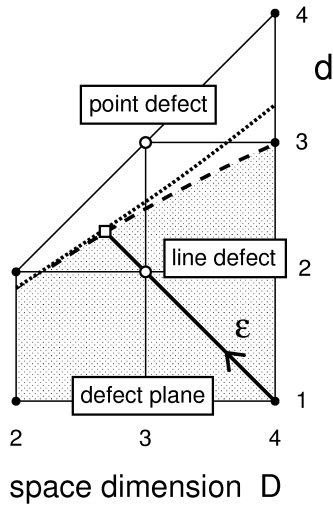


FIG. 2. Various types of defects in space dimension D and with internal dimension $D - d$: point defect ($d = D$), line defect ($d = 2$), and defect plane ($d = 1$). Within the shaded region below the dashed line $d = D - \beta/\nu$ the symmetry breaking field on the defect gives rise to critical adsorption. The dotted line is the approximation based on Eq. (2) for the dashed line. The path indicated by the arrow is used to calculate the critical exponents shown in Table I for a line defect in $D = 3$ [see Eq. (10)].

homogeneous bulk field. [The reasoning is similar to that of Ref. [4(b)] which leads to the prediction that for a (100) surface of an antiferromagnet in the presence of a homogeneous bulk field there is normal surface critical behavior.] The continuum description for a line defect is given by the standard Hamiltonian

$$\mathcal{H}\{\Phi\} = \int d^D r \left\{ \frac{1}{2} (\nabla\Phi)^2 + \frac{\tau}{2} \Phi^2 + \frac{u}{24} \Phi^4 - h\Phi \right\} \quad (3)$$

for a scalar order parameter field $\Phi(\mathbf{r})$. The position vector $\mathbf{r} \in \mathbb{R}^D$ is decomposed into $\mathbf{r} = (\mathbf{r}_{\parallel}, \mathbf{r}_{\perp})$, where \mathbf{r}_{\parallel} and \mathbf{r}_{\perp} comprise the $D - d$ components parallel and the d components perpendicular, respectively, to the line defect, which is located at $r_{\perp} = |\mathbf{r}_{\perp}| = 0$. Equation (3) is supplemented by the boundary condition $\Phi = +\infty$ at the defect corresponding to the critical adsorption fixed point. The temperature parameter $\tau \sim T - T_c$ is related to the bulk coupling K in Eq. (1) by $\tau \sim K^C - K$. The bulk field h is the continuum analog of H in Eq. (1). The critical exponents shown in Table I are defined in the same way as for a planar wall [2,3]: the two-point correlation function at bulk criticality, i.e., $\tau = h = 0$, along the line defect, i.e., $|\mathbf{r}_{\parallel} - \mathbf{r}'_{\parallel}| \rightarrow \infty$ with r_{\perp} and r'_{\perp} fixed, decays as

$$\langle \Phi(\mathbf{r})\Phi(\mathbf{r}') \rangle \sim |\mathbf{r}_{\parallel} - \mathbf{r}'_{\parallel}|^{-(D-2+\eta_{\parallel})}; \quad (4)$$

η_{\perp} is defined analogously for the case that the distance between the two points tends to infinity perpendicular to the defect, i.e., $|\mathbf{r}_{\perp} - \mathbf{r}'_{\perp}| \rightarrow \infty$ with r_{\parallel} fixed; the *line*

magnetization $M_1 = \langle \Phi(\mathbf{r}) \rangle$ (for \mathbf{r} close to the line defect) and the *layer susceptibility* $\chi_1 = \partial M_1 / \partial h$ behave as

$$[M_1 - M_1(\tau = 0)]_{\text{sing}} \sim |\tau|^{\beta_1},$$

$$\chi_1|_{\text{sing}} \sim |\tau|^{-\gamma_1}, \quad \tau \rightarrow 0, \quad h = 0;$$

$$[M_1 - M_1(h = 0)]_{\text{sing}} \sim |h|^{1/\delta_1}, \quad h \rightarrow 0, \quad \tau = 0, \quad (5)$$

where the subscript “sing” refers to the *leading singular parts* of M_1 and χ_1 [2,3]. The critical exponents for critical adsorption on a line defect are supposed to be attributed to the leading *line* operator σ in the short-distance expansion of the order parameter $\Phi(\mathbf{r})$ near the line defect:

$$\frac{\Phi(\mathbf{r})}{\langle \Phi(\mathbf{r}) \rangle} = I + b_{\sigma} r_{\perp}^{x_{\sigma}} \sigma(\mathbf{r}_{\parallel}) + \dots, \quad (6)$$

where the average $\langle \Phi(\mathbf{r}) \rangle$ is taken at the bulk critical point, I is the identity operator, and b_{σ} is an amplitude. The leading short-distance behavior of $\Phi(\mathbf{r})$ in correlation functions is dictated by the scaling dimension x_{σ} of σ . The short-distance expansion according to Eq. (6) is known to hold for critical adsorption on a planar wall for which the surface operator corresponding to σ turns out to be $\lim_{z \rightarrow 0} T_{zz}$ with z the distance from the wall and T_{zz} the stress-energy tensor [13]. For a planar wall the amplitude corresponding to b_{σ} is universal and one has (compare Fig. 2)

$$\eta_{\parallel} = D + 2, \quad 2 \leq D \leq 4, \quad d = 1. \quad (7)$$

Both can be traced back to the fact that the stress-energy tensor does not need to be renormalized at the wall so that its scaling dimension equals its canonical inverse length dimension D [13,14]. For a line defect instead of a planar wall the explicit form of the operator $\sigma(\mathbf{r}_{\parallel})$ in Eq. (6) is presently unknown. Equation (6) provides, however, important and checkable conclusions: (i) only *one* new singularity, which is characterized by the scaling dimension x_{σ} of $\sigma(\mathbf{r}_{\parallel})$, shows up; (ii) all critical exponents for critical adsorption on a line defect shown in Table I can be expressed in terms of $\eta_{\parallel} = 2 - D + 2x_{\sigma}$ and bulk critical exponents η , ν , β , and δ via the same scaling relations as for a planar wall, i.e.,

$$\begin{aligned} \eta_{\perp} &= \frac{1}{2} (\eta + \eta_{\parallel}), & \beta_1 &= \frac{\nu}{2} (D - 2 + \eta_{\parallel}), \\ \gamma_1 &= \nu(2 - \eta_{\perp}), & \delta_1 &= \delta\beta/\beta_1. \end{aligned} \quad (8)$$

In addition to Eq. (7), within mean-field theory the critical exponents are available for *arbitrary* values of d . For example, at the critical adsorption fixed point the order parameter profile $m(r_{\perp}) = \sqrt{u/6} \langle \Phi(\mathbf{r}) \rangle$ corresponding to Eq. (3) which solves the mean-field equation $m'' + (d-1)m'/r_{\perp} = m^3$ is given by $m(r_{\perp}) = \sqrt{3-d}/r_{\perp}$ for $1 \leq d < 3$ [12]. This underscores that there exists a long-range critical adsorption profile for $D = 4$, $1 \leq d < 3$ (see Fig. 2). The two-point correlation function $\langle \Phi(\mathbf{r})\Phi(\mathbf{r}') \rangle$ for Gaussian fluctuations

around this profile can be derived by standard methods [2,3]. Using Eq. (4) one finds

$$\eta_{\parallel} = 2 - d + \sqrt{40 - 16d + d^2}, \quad D = 4, \\ 1 \leq d < 3, \quad (9)$$

and $\eta_{\perp} = \eta_{\parallel}/2$, in accordance with the first scaling relation in Eq. (8) where $\eta = 0$ in $D = 4$. The mean-field values for the remaining critical exponents β_1 , γ_1 , and δ_1 can be derived *independently* from one another, resulting in expressions valid for $1 \leq d < 3$ at $D = 4$ similar to Eq. (9). It turns out that all scaling relations in Eq. (8) are fulfilled on the whole line $D = 4$, $1 \leq d < 3$. Table I shows the corresponding values for a line defect, i.e., $D = 4$ and $d = 2$.

The knowledge of η_{\parallel} on the lines ($D, d = 1$) and ($D = 4, d$) [see Eqs. (7) and (9)] in conjunction with the fact that $\eta_{\parallel} = \eta$ on the line $d = D - \beta/\nu$ (dashed line in Fig. 2) can be used to derive a rather accurate estimate for η_{\parallel} for a line defect in $D = 3$. Assuming that η_{\parallel} as a function of D and d forms a regular surface over the (D, d) plane within the shaded region in Fig. 2, Eqs. (7) and (9) determine the plane tangent to this $\eta_{\parallel}(D, d)$ surface at $(D, d) = (4, 1)$. This yields, in particular, the following ε expansion of η_{\parallel} to first order in $\varepsilon = 4 - D$:

$$\eta_{\parallel} = 6 - \frac{17}{5} \varepsilon + \mathcal{O}(\varepsilon^2), \quad D = 4 - \varepsilon, \\ d = 1 + \varepsilon. \quad (10)$$

The corresponding path on the (D, d) plane is indicated by the arrow in Fig. 2. This path intersects the point (3, 2) corresponding to a line defect in $D = 3$ and ends at the value $D_0 = 2.690 \pm 0.005$ [11] of the space dimension D (open square in Fig. 2) where $\eta_{\parallel} = \eta(D_0)$. The bulk value $\eta(D_0) = 0.074 \pm 0.005$ and Eq. (10) determine the coefficients a_i and b_i in interpolation schemes for η_{\parallel} in the form of a polynomial to second order in ε , i.e., $\eta_{\parallel} = a_0 + a_1\varepsilon + a_2\varepsilon^2$, and of a (1, 1)-Padé form in ε , i.e., $\eta_{\parallel} = b_0 + b_1\varepsilon/(1 + b_2\varepsilon)$, respectively. The value of η_{\parallel} shown in Table I for a line defect in $D = 3$ is the mean value of these two interpolation schemes for $\varepsilon = 1$, while the indicated error has been obtained from the difference between the two values [15]. The values of the critical exponents η_{\perp} , β_1 , and γ_1 shown in Table I for a line defect in $D = 3$ have been obtained *independently* using the above described method: Their known expansions in $\varepsilon = 4 - D$ for $d = 1$ (planar wall) were combined with their expansions in $d - 1$ for $D = 4$ (mean field) [compare Eqs. (7), (9), and (10)], and then both interpolation schemes were applied to each of them. The fact that the first three scaling relations in Eq. (8) are fulfilled within the error bars underscores the reliability of this method.

For the value of δ_1 shown in Table I the last scaling relation in Eq. (8) has been used.

Table I shows that the thermodynamic singularities for a line defect are more pronounced than for a planar wall. For example, χ_1 *diverges* for $\tau \rightarrow 0$ in the case of a line defect, whereas no such divergence occurs for a planar wall; similarly, the τ derivative of M_1 *diverges* for $\tau \rightarrow 0$ for a line defect but not for a planar wall. Of course, it is desirable to clarify the nature of the singularities and to identify the line operator σ in Eq. (6). The estimates for the critical exponents, however, should be accurate enough for meaningful tests.

The author is grateful to F. Schlesener for helpful assistance. This work was supported by the German Science Foundation through Sonderforschungsbereich 237.

*Present address: Department of Physics, MIT, Cambridge, MA 02139.

- [1] M. E. Fisher, *Rev. Mod. Phys.* **46**, 597 (1974); **70**, 653 (1998).
- [2] K. Binder, in *Phase Transitions and Critical Phenomena*, edited by C. Domb and J. L. Lebowitz (Academic, London, 1983), Vol. 8, p. 1.
- [3] H. W. Diehl, in *Phase Transitions and Critical Phenomena*, edited by C. Domb and J. L. Lebowitz (Academic, London, 1986), Vol. 10, p. 75; H. W. Diehl, *Int. J. Mod. Phys. B* **11**, 3503 (1997).
- [4] (a) F. Schmid, *Z. Phys. B* **91**, 77 (1993); (b) A. Drewitz, R. Leidl, T. W. Burkhardt, and H. W. Diehl, *Phys. Rev. Lett.* **78**, 1090 (1997).
- [5] L. Mailänder, H. Dosch, J. Peisl, and R. L. Johnson, *Phys. Rev. Lett.* **64**, 2527 (1990); B. Burandt, W. Press, and S. Haussühl, *Phys. Rev. Lett.* **71**, 1188 (1993); S. Krimmel, W. Donner, B. Nickel, H. Dosch, C. Sutter, and G. Grübel, *Phys. Rev. Lett.* **78**, 3880 (1997).
- [6] *Physics of Defects*, edited by R. Balian, M. Kléman, and J.-P. Poirier (North-Holland, Amsterdam, 1981).
- [7] F. Iglói, I. Peschel, and L. Turban, *Adv. Phys.* **42**, 683 (1993).
- [8] M. V. Belousov and B. E. Vol'f, *JETP Lett.* **31**, 317 (1980).
- [9] A. A. Migdal, *Sov. Phys. JETP* **42**, 743 (1975); L. P. Kadanoff, *Ann. Phys. (N.Y.)* **100**, 359 (1976).
- [10] R. Lipowsky and H. Wagner, *Z. Phys. B* **42**, 355 (1981).
- [11] The values of $\beta(D)$ and $\nu(D)$ are known quite accurately by high-order ε expansions in conjunction with Borel summation techniques. See R. Guida and J. Zinn-Justin, *J. Phys. A* **31**, 8103 (1998).
- [12] A. Hanke and S. Dietrich, *Phys. Rev. E* **59**, 5081 (1999).
- [13] J. L. Cardy, *Phys. Rev. Lett.* **65**, 1443 (1990).
- [14] E. Eisenriegler and M. Stapper, *Phys. Rev. B* **50**, 10009 (1994).
- [15] Compare Fig. 3 and the related discussion in A. Hanke, E. Eisenriegler, and S. Dietrich, *Phys. Rev. E* **59**, 6853 (1999); G. Flöter and S. Dietrich, *Z. Phys. B* **97**, 213 (1995).